

Factorized approach to radiative corrections for inelastic lepton-hadron collisions

Tianbo Liu, W. Melnitchouk, Jian-Wei Qiu, and N. Sato
Theory Center, Jefferson Lab, Newport News, Virginia 23606, USA

We propose a new factorized approach to QED radiative corrections (RCs) in inclusive and semi-inclusive lepton-hadron deep-inelastic scattering. The method allows the systematic resummation of the logarithmically enhanced RCs into factorized lepton distribution and fragmentation (or jet) functions that are universal for all final states. The new approach provides a uniform treatment of RCs for the extraction of parton distribution functions, transverse momentum dependent distributions, and other partonic correlation functions from lepton-hadron collision data.

Introduction.— Lepton-hadron deep-inelastic scattering (DIS) has played a critical role in the development of our understanding of the strong nuclear force and the internal structure of nucleons and nuclei, since the first such experiments were performed at SLAC over 50 years ago [1]. By measuring the momentum transfer, $q \equiv \ell - \ell'$, from an incident lepton with momentum ℓ scattered to a lepton with momentum ℓ' , and keeping $Q \equiv \sqrt{-q^2} \gg 1/R$, where R is the hadron radius [see Fig. 1(a)], the DIS experiments provided a short-distance electromagnetic probe of the point-like quarks inside hadrons, ultimately giving birth to QCD as the fundamental theory of strong interactions. Without observing specific final states other than the scattered lepton, this modern version of Rutherford scattering provided the first glimpse of the hadrons' internal landscape of quarks and gluons (or collectively, partons), parametrized through the parton distribution functions (PDFs) as probability densities for finding a parton inside the hadron with momentum fraction x [2]. While our discussion applies to any hadronic initial state, for clarity we will specialize to the case of a nucleon in the rest of the paper.

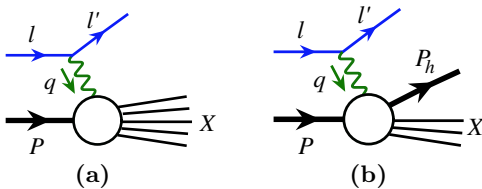


FIG. 1. Inelastic scattering of a lepton (ℓ) from a nucleon (P) to a scattered lepton (ℓ') via exchange of a photon (q) for (a) inclusive final states X , and (b) semi-inclusive production of a hadron (P_h).

By detecting a hadron (or jet) of momentum P_h in the final state [Fig. 1(b)], this semi-inclusive DIS (SIDIS) process has two naturally ordered momentum scales: Q , and the transverse momentum $P_{hT} \ll Q$, defined in a frame where the virtual photon collides with the nucleon moving along the z -axis. While the hard scale Q localizes the probe to resolve the partons' longitudinal momentum distributions, the soft scale $P_{hT} \gtrsim 1/R$ provides the sensitivity needed to probe the partons' transverse mo-

tion inside the colliding nucleon. With the leptonic plane defined by ℓ and ℓ' and the hadronic plane by P and P_h , different angular modulations between these planes in SIDIS allow the extraction of various transverse momentum dependent distributions (TMDs), which encode rich information about the nucleon's three-dimensional landscape in momentum space [3–7].

In practice, the collision with a large momentum transfer triggers radiation of photons, such as those from the colliding and scattered leptons and quarks illustrated in Fig. 2. This radiation not only changes the momentum transfer q , making it problematic to define the exact photon-nucleon frame, but also alters the angular modulation between the leptonic and hadronic planes. Reliable extraction of PDFs and TMDs requires such collision-induced QED radiation to be taken into account in the form of radiative corrections (RCs) [8]. Without being able to account for all radiated photons experimentally, some of the RCs rely on measurement of the invariant mass of the hadronic final state and Monte Carlo simulation [9–12], which introduces model dependence into the purely leptonic part of the radiation in Fig. 2.

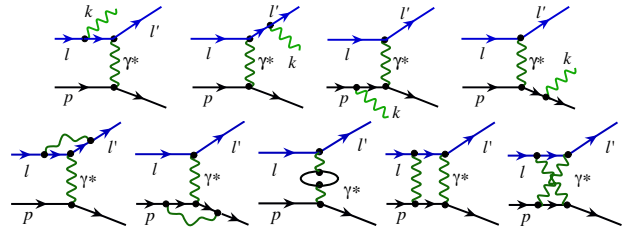


FIG. 2. Diagrams for the first real (top row) and virtual (bottom row) RCs to scattering of a lepton (momentum ℓ) from a quark (p) to a lepton (ℓ') and recoiling quark.

In this Letter, we propose a new factorization approach to QED radiation in lepton-nucleon scattering, with or without observation of specific hadrons in the final state. Instead of treating QED radiation as a correction to the Born process [13, 14], which becomes increasingly difficult beyond inclusive DIS [15–17], we unify the QED and QCD contributions in a consistent factorization formalism. The new approach allows all collinear (CO) sensitive and logarithmically-enhanced photon radiation to be systematically resummed into factorized, either CO

or TMD, universal lepton distribution functions (LDFs) and lepton fragmentation (or jet) functions (LFFs), or as QED modifications to the evolution of nucleon PDFs or TMDs. The remainder of the QED contributions are then insensitive to lepton mass $m_e \rightarrow 0$, and included in the infrared (IR) safe, perturbatively calculable hard parts, plus corrections suppressed by powers of m_e over the hard scale of the collisions. Similar ideas have been explored in the context of e^+e^- reactions [18–20]. Calculating RCs is then replaced by determining the universal LDFs and LFFs, along with perturbative calculation of IR-safe QED corrections to the short-distance hard parts. With both QCD and QED factorization, the new framework provides a consistent and perturbatively stable strategy to extract PDFs and TMDs from lepton-nucleon scattering.

Inclusive lepton-nucleon DIS.— In the absence of photon radiation from the leptons, and dropping lepton and hadron masses, the spin-averaged inclusive cross section for the lepton-nucleon DIS process in Fig. 1(a), $e(\ell) + N(P) \rightarrow e(\ell') + X$, is given by

$$\begin{aligned} E' \frac{d\sigma_{\text{DIS}}}{d^3\ell'} &= \frac{\alpha^2}{2\pi s} \sum_X \left| \langle \ell' | j_\mu | \ell \rangle \frac{1}{q^2} \langle X | J^\mu | P \rangle \right|^2 \\ &\times (2\pi)^4 \delta^{(4)}(P + q - X) \\ &= \frac{4\alpha^2}{s x_B y^2 Q^2} \left[x_B y^2 F_1(x_B, Q^2) + (1-y) F_2(x_B, Q^2) \right], \end{aligned} \quad (1)$$

where $\alpha = e^2/4\pi$ is the electromagnetic fine structure constant, j_μ (J_μ) is the lepton (quark) current, and the kinematic variables are given by $s = (P + \ell)^2$, $Q^2 = -(\ell - \ell')^2 > 0$, $x_B = Q^2/2P \cdot q$, and $y = P \cdot q/P \cdot \ell$. The structure functions F_1 and F_2 carry information about the nucleon’s substructure, and can be factorized in terms of PDFs with corrections suppressed by powers of $1/Q^2$ [21]. The inclusive cross section in Eq. (1) would provide a clean probe of F_1 and F_2 [22–28].

However, in the presence of photon radiation F_1 and F_2 are not direct physical observables. Without accounting for all photon radiation, the exchanged photon momentum q cannot be determined exactly, which impacts the extraction of PDFs. With the small m_e , photon radiation could be enhanced by $\ln(Q^2/m_e^2)$, leading to large, but not precisely determined, RCs that are sensitive to kinematic variables such as x_B and Q^2 . The factorization approach proposed in this work, while unable to ensure the extraction of F_1 and F_2 , does nevertheless provide a perturbatively stable formalism for the reliable extraction of PDFs from inclusive DIS cross sections.

We consider the inclusive DIS cross section in Eq. (1) for a lepton scattered with a large transverse component $\ell'_T \gg \Lambda_{\text{QCD}}$ in the colliding lepton-nucleon frame. Applying the factorization formalism for single-hadron production at large transverse momentum in hadronic collisions [29] to lepton-nucleon scattering, the factorized DIS

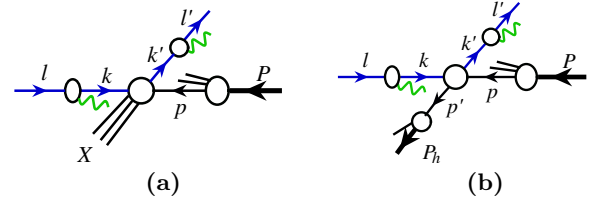


FIG. 3. Sketch of scattering amplitudes for (a) the factorized DIS process in (2), and (b) SIDIS with a “hard” scale $\ell'_T \sim P_{hT} \gg \Lambda_{\text{QCD}}$ and a “soft” scale $|\ell'_T + P_{hT}| \ll \ell'_T$.

cross section can be written [Fig. 3(a)],

$$\begin{aligned} E' \frac{d\sigma_{\text{DIS}}}{d^3\ell'} &= \frac{1}{2s} \sum_{i,j,a} \int_{z_L}^1 \frac{d\zeta}{\zeta^2} \int_{x_L}^1 \frac{d\xi}{\xi} D_{e/j}(\zeta) f_{i/e}(\xi) \\ &\times \int_{x_h}^1 \frac{dx}{x} f_{a/N}(x) \widehat{H}_{ia \rightarrow j}(\xi, \zeta, x; k') + \dots \end{aligned} \quad (2)$$

where i, j, a include all QED and QCD particles [30]. The lower limits z_L, x_L and x_h depend on external kinematics as specified below, and the ellipsis represents power corrections suppressed by $1/\ell'^2_T$. In Eq. (2), the LDF $f_{i/e}(\xi)$ gives the probability to find lepton i with light-cone momentum $\xi\ell^+$ in the incident lepton e [31],

$$f_{i/e}(\xi) = \int \frac{dz^-}{4\pi} e^{i\xi\ell^+z^-} \langle e | \bar{\psi}_i(0) \gamma^+ \Phi_{[0, z^-]} \psi_i(z^-) | e \rangle, \quad (3)$$

where $\Phi_{[0, z^-]} = \exp[-ie \int_0^{z^-} d\eta^- A^+(\eta^-)]$ is the gauge link with photon field A^μ , and we use light-cone notation $v^\pm = (v^0 \pm v^3)/\sqrt{2}$ for any four-vector v^μ . Similarly, the LFF $D_{e/j}(\zeta)$ describes the emergence of the final lepton e of momentum ℓ' from lepton j of momentum $\sim \ell'/\zeta$,

$$\begin{aligned} D_{e/j}(\zeta) &= \frac{\zeta}{2} \sum_X \int \frac{dz^-}{4\pi} e^{i\ell'^+z^-/\zeta} \\ &\times \text{Tr}[\gamma^+ \langle 0 | \bar{\psi}_j(0) \Phi_{[0, \infty]} | e, X \rangle \langle e, X | \psi_j(z^-) \Phi_{[z^-, \infty]} | 0 \rangle], \end{aligned} \quad (4)$$

where the plus direction is defined as $\ell' = (\ell'^+, 0^-, \mathbf{0}_T)$, while the plus direction in (3) is defined along ℓ . Both the LDF (3) and LFF (4) are defined in analogy with the quark PDF in the nucleon, $f_{a/N}(x)$, where $x = p^+/P^+$ is the nucleon momentum fraction carried by the quark, and quark to hadron fragmentation function [32], with the quark and gluon fields replaced by lepton and photon fields, and the hadron state by a lepton state.

In Eq. (2), the $\widehat{H}_{ia \rightarrow j}$ is lepton-parton scattering cross section with all logarithmic CO sensitivities along the direction of observed momenta, ℓ, ℓ' and P , removed, and is therefore IR safe and insensitive to taking $m_e \rightarrow 0$. The IR-safe $\widehat{H}_{ia \rightarrow j}$ can be perturbatively calculated by expanding the factorized formula (2) order-by-order in powers of α and α_s , with $\widehat{H}_{ia \rightarrow j}^{(m,n)}$ denoting the contribution at $\mathcal{O}(\alpha^m \alpha_s^n)$. The factorized inclusive DIS cross section in Eq. (2) resums large photon radiation collinearly

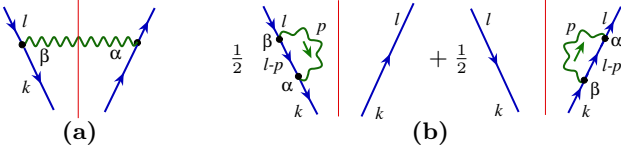


FIG. 4. Real (a) and virtual (b) QED diagrams contributing to the NLO LDF $f_{e/e}^{(1)}$.

sensitive to the incident lepton into $f_{i/e}$, and radiation that is collinearly sensitive to the scattered lepton into $D_{e/j}$, and takes care of the photon radiation collinear to the colliding nucleon by adding QED corrections to the evolution kernels of the nucleon PDF $f_{a/N}$.

QED contributions.— As for the factorized QCD case, the QED contribution to inclusive eN scattering is organized into CO sensitive LDFs and LFFs, and IR-safe hard scattering functions. Unlike the PDFs in QCD, however, which are nonperturbative, LDFs are calculable perturbatively in QED. Focusing for brevity only on the “valence” lepton part [$i = j = e$ in Eq. (2)], at leading order (LO) in α we have, from Eq. (3), $f_{e/e}^{(0)}(\xi) = \delta(\xi - 1)$. At next-to-leading order (NLO), the real and virtual contribution in the light-cone gauge are given by the diagrams in Fig. 4(a) and (b), respectively, leading to

$$f_{e/e}^{(1)}(\xi, \mu^2) = \frac{\alpha}{2\pi} \left[\frac{1 + \xi^2}{1 - \xi} \ln \frac{\mu^2}{(1 - \xi)m_e^2} \right]_+, \quad (5)$$

where μ^2 is the factorization scale defined under the $\overline{\text{MS}}$ renormalization scheme, and the standard “+” prescription is used. As with PDFs, high-order contributions to LDFs can be systematically resummed by solving the evolution equations for QED particles [33–38],

$$\mu^2 \frac{d}{d\mu^2} f_{e/e}(\xi, \mu^2) = \int_{\xi}^1 \frac{d\xi'}{\xi'} P_{ee}(\xi/\xi', \alpha) f_{e/e}(\xi', \mu^2), \quad (6)$$

with evolution kernels P_{ee} calculable perturbatively at a given order in α . At $\mathcal{O}(\alpha)$, from Eq. (5) we have $P_{ee}^{(1)}(z, \alpha) = (\alpha/2\pi) [(1+z^2)/(1-z)]_+$.

Similarly, the LFFs can also be calculated perturbatively in QED, which at LO are given by $D_{e/e}^{(0)}(\zeta) = \delta(\zeta - 1)$, and at $\mathcal{O}(\alpha)$ in the $\overline{\text{MS}}$ scheme by

$$D_{e/e}^{(1)}(\zeta, \mu) = \frac{\alpha}{2\pi} \left[\frac{1 + \zeta^2}{1 - \zeta} \ln \frac{(1 - \zeta)\mu^2}{\Delta E^2} \right]_+, \quad (7)$$

where ΔE^2 is the invariant mass resolution of the radiated photon ($\Delta E^2 = 0.01 \text{ GeV}^2$ is used in our numerical study). The higher-order contributions to the LFFs can be resummed by solving the corresponding evolution equations. Power corrections in m_e^2/μ^2 and $\Delta E^2/\mu^2$ are neglected in deriving Eqs. (5) and (7).

To compute the IR-safe hard part in Eq. (2), we replace the target nucleon by a point-like quark target q . The

lepton-quark cross section can then be expanded to a given order in α and α_s , with the $\mathcal{O}(\alpha^m \alpha_s^n)$ contribution denoted by $\sigma_{eq}^{(m,n)} \equiv 2sE' d\sigma_{eq \rightarrow eX}/d^3\ell'$. Expanding to lowest order [$\mathcal{O}(\alpha^2 \alpha_s^0)$], we have

$$\sigma_{eq}^{(2,0)} = D_{e/e}^{(0)} \otimes f_{e/e}^{(0)} \otimes f_{q/q}^{(0)} \otimes \widehat{H}_{eq \rightarrow e}^{(2,0)} = \widehat{H}_{eq \rightarrow e}^{(2,0)}, \quad (8)$$

where \otimes indicates the convolution of momentum fractions, and the $\mathcal{O}(\alpha_s^0)$ quark distribution $f_{q/q}^{(0)}(x) = \delta(x-1)$ is also used. Evaluating the lowest order lepton-quark scattering diagram, one finds for the hard function

$$\widehat{H}_{eq \rightarrow e}^{(2,0)} = 4\alpha^2 e_q^2 \left(\frac{\hat{s}^2 + \hat{u}^2}{\hat{t}^2} \right) \delta(\hat{s} + \hat{t} + \hat{u}), \quad (9)$$

where the partonic Mandelstam variables are $\hat{s} = x\xi s$, $\hat{t} = (\xi/\zeta)t$, and $\hat{u} = (x/\zeta)u$, with the observed Mandelstam variables $s = (P + \ell)^2$, $t = (\ell - \ell')^2 = -Q^2$, and $u = (P - \ell')^2 = -(1-y)s$. Substituting the calculated $\widehat{H}_{eq \rightarrow e}^{(2,0)}$ into Eq. (2), we have

$$E' \frac{d\sigma_{\text{DIS}}}{d^3\ell'} \approx \frac{2\alpha^2}{s} \sum_q \int_{z_L}^1 \frac{d\zeta}{\zeta^2} \int_{x_L}^1 \frac{d\xi}{\xi} D_{e/e}(\zeta) f_{e/e}(\xi) \times \int_{x_h}^1 \frac{dx}{x} e_q^2 f_{q/N}(x) \frac{x^2 \zeta [(\xi\zeta s)^2 + u^2]}{(\xi t)^2 (\xi\zeta s + u)} \delta(x - x_h), \quad (10)$$

where the integral limits are given by $z_L = -(t+u)/s$, $x_L = -u/(\zeta s + t)$, and $x_h = -\xi t/(\xi\zeta s + u)$. Choosing $f_{e/e}(\xi) \approx f_{e/e}^{(0)}(\xi)$ and $D_{e/e}(\zeta) \approx D_{e/e}^{(0)}(\zeta)$ in Eq. (10), and noting that to $\mathcal{O}(\alpha_s^0)$ the structure functions in Eq. (1) are given by $F_2(x_B) = 2x_B F_1(x_B) = \sum_q e_q^2 x_B f_{q/N}(x_B)$, one can reproduce the lepton-nucleon cross section in Eq. (1) from Eq. (10). The key difference between Eqs. (1) and (10), apart from IR-safe high order QED contribution, is the resummation of logarithmic-enhanced photon radiation for the colliding and scattered leptons into the LDFs and LFFs, respectively.

With the factorization formalism in Eq. (2), one can systematically improve the “RCs” by calculating the IR-safe hard parts $\widehat{H}_{eq \rightarrow e}^{(m,n)}$ perturbatively for $m > 2$, and determining the lepton mass-sensitive, but universal, LDFs and LFFs. For example, at $m = 3$ one can write

$$\widehat{H}_{eq \rightarrow e}^{(3,0)} = \sigma_{eq}^{(3,0)} - D_{e/e}^{(1)} \otimes \widehat{H}_{eq \rightarrow e}^{(2,0)} - f_{e/e}^{(1)} \otimes \widehat{H}_{eq \rightarrow e}^{(2,0)} - f_{q/q}^{(1)} \otimes \widehat{H}_{eq \rightarrow e}^{(2,0)} - f_{\gamma/q}^{(1)} \otimes \widehat{H}_{e\gamma \rightarrow e}^{(2,0)}, \quad (11)$$

where $\sigma_{eq}^{(3,0)}$ is given by the diagrams in Fig. 2, and the three subtraction terms involve convolutions over different momentum fractions to remove the collinear-sensitive photon radiation from the scattered lepton, incident lepton, and incident quark, respectively. With IR safety, the perturbatively calculated RCs are completely perturbative-stable and insensitive to the lepton mass $m_e \rightarrow 0$, with all m_e -sensitive RCs resummed into universal LDFs and LFFs.

Numerical impact.— In general, the larger the momentum transfer Q^2 , or more available phase space $s \gg Q^2$, the more important are the RCs. In our factorization approach, the logarithmically enhanced RCs are included in the universal LDFs and LFFs, which shift the momenta of active leptons, and consequently impact the momentum transfer to the colliding nucleon. To demonstrate the numerical impact of RCs, we show in Fig. 5 the ratio of the DIS cross sections $\sigma \equiv E'd\sigma_{\text{DIS}}/d^3\ell'$ without RCs (“ σ_{noRC} ”) and including RCs (“ σ_{RC} ”), where σ_{noRC} is given by Eq. (10) with $f_{e/e} \rightarrow f_{e/e}^{(0)}$ and $D_{e/e} \rightarrow D_{e/e}^{(0)}$. The cross section σ_{RC} is also given by Eq. (10) but evaluated with (i) NLO: $f_{e/e} = f_{e/e}^{(0)} + f_{e/e}^{(1)}$ and $D_{e/e} = D_{e/e}^{(0)} + D_{e/e}^{(1)}$, (ii) RES_I: resummed (or evolved) LDF and LFF with input distribution $f_{e/e} = f_{e/e}^{(0)}$ and $D_{e/e} = D_{e/e}^{(0)}$ at $\mu_0^2 = m_c^2$, or (iii) RES_{II}: resummed LDF and LFF with input $f_{e/e} = f_{e/e}^{(0)} + f_{e/e}^{(1)}$ and $D_{e/e} = D_{e/e}^{(0)} + D_{e/e}^{(1)}$.

The factorization scales for the LDFs and PDFs are chosen to be $\max[m_c^2, -t]$, where m_c is the charm quark mass, to guarantee the factorization theorem to hold. Scale variations of the form $\max[m_c^2, w_1\ell_T^2 - w_2t]$, with $(w_1, w_2) = (1, 0)$ and $(\frac{1}{2}, \frac{1}{2})$, were found to give relatively weak dependence on the scale choices, confirming the stability of our results in Fig. 5. For the PDFs in the nucleon we use the parametrizations from the recent JAM global QCD analysis [39], but the results with other PDF sets [40] are almost indistinguishable.

The results in Fig. 5, shown for kinematics typical of Jefferson Lab (JLab) experiments and those planned for the Electron-Ion Collider (EIC), illustrate some surprising and rather dramatic effects of RCs in certain regions of phase space. Defining $y_{\ell'}$ to be the scattered lepton rapidity, the ratio $\sigma_{\text{noRC}}/\sigma_{\text{RC}}$ versus ℓ_T' was shown for several fixed values of $y_{\ell'}$ typical for JLab [Fig. 5(a)] and EIC [Fig. 5(b)] kinematics. The general trend of the effects is an increase in the magnitude of the correction at lower ℓ_T' , consistent with more phase space available for photon radiation. With the greater phase space available at the EIC, the RC effects can become quite significant at lower ℓ_T' values, even with $\ell_T' > 1$ GeV, and the differences between the RC prescriptions (NLO, RES_I or RES_{II}) become more evident. While the differences between the NLO and resummed results can be large, the differences between the two resummed versions, RES_I and RES_{II}, are much smaller. This suggests that the resummation effects are important and the uncertainty in choosing the input distributions is mild, which provides greater stability in our factorization approach to calculate QED contribution to inelastic lepton-hadron scattering.

The impact of the RCs can be more directly visualized in terms of the traditional DIS variables x_B and Q^2 , and in Fig. 5(c)–(d) the ratio $\sigma_{\text{noRC}}/\sigma_{\text{RC}}$ is shown versus x_B at fixed Q^2 . The most striking feature for both JLab and EIC kinematics is the dramatic change of slope in the x_B

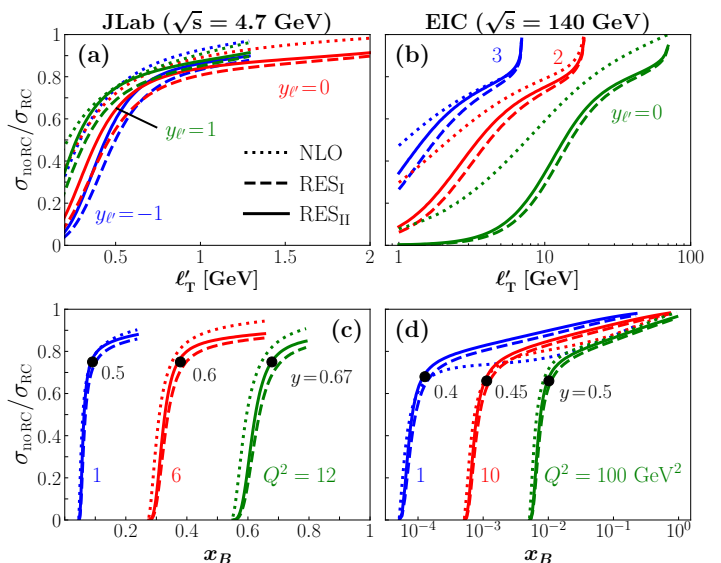


FIG. 5. Ratios of inclusive ep cross sections with no RCs to those including RCs computed according to the NLO (dotted lines), RES_I (dashed lines), and RES_{II} (solid lines) schemes, referred to in the text. The values of y at which the RCs are $\gtrsim 30\%$ are marked by the black filled circles.

dependence, from relatively shallow at higher x_B , where the RCs are $\lesssim 20\%$, to a steep fall-off with decreasing x_B , where the RCs overwhelm the Born contribution as $x_B \rightarrow x_B^{\text{min}} = Q^2/s$ when $y \rightarrow 1$. For JLab kinematics this turnover occurs when $y \approx 0.5 - 0.6$, depending on the Q^2 value, but at even smaller values, $y \approx 0.4$, for EIC kinematics. Note that a cut on the final state hadronic mass (> 2 GeV) is made to avoid the nucleon resonance region, which restricts the maximum value of x_B that can be reached at fixed Q^2 . Our results in Fig. 5 clearly indicate that extreme care should be taken when extracting partonic information from data on inclusive DIS cross section at low x_B and high Q^2 , in view of the potentially large uncertainties in the QED RCs.

Semi-inclusive DIS.— Turning now to the SIDIS process, $eN \rightarrow ehX$, depicted in Fig. 1(b), the observed leading hadron naturally has a small transverse momentum in the Breit frame (or in a general “photon-hadron” frame), which makes the SIDIS to be sensitive to the transverse momentum of the colliding parton, and permits a description in terms of TMDs. However, as shown in Fig. 2, the virtual photon momentum q is not directly measured, and can be determined only if one can account for all induced photon radiation, meaning that in practice the photon-hadron frame is not precisely defined.

Without attempting to identify the “virtual” photon, we can define SIDIS as an inclusive lepton-nucleon scattering process to produce a scattered lepton of momentum ℓ' and a leading hadron (or a jet) of momentum P_h . In the plane transverse to the lepton-nucleon collision in

the lab frame, the scattered lepton and produced hadron are likely to be back-to-back. Introducing

$$\bar{\mathbf{P}}_T \equiv \frac{1}{2}(\ell'_T - \mathbf{p}_{hT}), \quad \bar{\mathbf{p}}_T \equiv \ell'_T + \mathbf{p}_{hT}, \quad (12)$$

for kinematics where $|\bar{\mathbf{P}}_T| \gg |\bar{\mathbf{p}}_T|$ one requires TMD factorization, while when $|\bar{\mathbf{P}}_T| \sim |\bar{\mathbf{p}}_T|$ the CO factorization is more relevant. The matching between the regimes where these two factorizations are applicable has been a topic of considerable recent interest [5, 41–43].

To formulate the TMD factorization for the SIDIS cross section in our new framework, we introduce a “parton frame” by a boost along the lepton-nucleon collision axis such that $y_{\ell'} + y_h = 0$, where $y_{\ell'}$ and y_h are the lab frame rapidities of the observed lepton and hadron, respectively. In this frame the observed lepton and the hadron are almost back-to-back, as shown in Fig. 3(b), which allows us to define

$$\frac{d\sigma_{\text{SIDIS}}}{dy_{\ell'} dy_h d^2\bar{\mathbf{P}}_T d^2\bar{\mathbf{p}}_T} = \frac{1}{2s} \sum_{i,j,a,b} \tilde{f}_{i/e} \otimes \tilde{D}_{e/j} \otimes \tilde{f}_{a/N} \otimes \tilde{D}_{h/b} \otimes \hat{H}_{ia \rightarrow jb}, \quad (13)$$

where $\hat{H}_{ia \rightarrow jb}$ is the hard function for producing a lepton j and parton b , with all CO sensitivity removed. The convolutions in (13) are in both CO momentum fraction and parton transverse momentum, and \tilde{f} and \tilde{D} denote incident particle TMDs defined with CO momentum along the lepton-nucleon collision axis, and outgoing particle TMDs with CO momentum along the observed lepton and hadron direction in the parton frame, respectively. Corrections to the factorized formula (13) are suppressed by powers of $(|\bar{\mathbf{p}}_T|/|\bar{\mathbf{P}}_T|)$. Further applications to SIDIS cross sections will be presented in Ref. [44].

Outlook — Our unified factorization approach to QED and QCD dynamics has important implications for future analyses of hard scattering at the EIC. Our observation that, without being able to account for all radiation, the photon-hadron frame is not well-defined and the standard x_B and Q^2 does not fully control the momentum transfer to the colliding hadron, could impact the precision with which one can extract TMDs and explore the nucleon’s 3-dimensional landscape in momentum space.

On the other hand, our unified factorization approach allows the systematic resummation of the logarithmically enhanced RCs into factorized LDFs and LFFs that are universal for all final states, leaving the fixed order QED corrections completely IR-safe and stable as $m_e \rightarrow 0$. In contrast to previous treatments of RCs computed for different observables, the new paradigm allows a uniform treatment of QED RCs for the extraction of parton distribution functions, transverse momentum dependent distributions and other partonic correlation functions from lepton-hadron collision data.

We thank the participants of the *Theory-Experiment Dialogue* at Jefferson Lab, A. Accardi, H. Avakian, J.-P. Chen, R. Ent, C. E. Keppel, T. C. Rogers and P. Rossi, for helpful discussions. This work is supported by the U.S. Department of Energy contract DE-AC05-06OR23177, under which Jefferson Science Associates, LLC, manages and operates Jefferson Lab, and within the framework of the TMD Topical Collaboration.

-
- [1] E. D. Bloom *et al.*, *Phys. Rev. Lett.* **23**, 930 (1969).
 - [2] R. P. Feynman, *Photon Hadron Interactions*, Benjamin, Reading, Massachusetts (1972).
 - [3] A. Bacchetta, M. Diehl, K. Goeke, A. Metz, P. J. Mulders and M. Schlegel, *J. High Energy Phys.* **02** (2007) 093.
 - [4] R. Angeles-Martinez *et al.*, *Acta Phys. Polon. B* **46**, 2501 (2015).
 - [5] J. Collins, L. Gamberg, A. Prokudin, T. C. Rogers, N. Sato and B. Wang, *Phys. Rev. D* **94**, 034014 (2016).
 - [6] M. Diehl, *Eur. Phys. J. A* **52**, 149 (2016).
 - [7] D. Gutierrez-Reyes, I. Scimemi, W. J. Waalewijn and L. Zoppi, *J. High Energy Phys.* **10** (2019) 031.
 - [8] B. Badelek, D. Y. Bardin, K. Kurek and C. Scholz, *Z. Phys. C* **66**, 591 (1995).
 - [9] K. Charchula, G. A. Schuler and H. Spiesberger, *Comp. Phys. Comm.* **81**, 381 (1994).
 - [10] N. Pierre, *Multiplicities of hadrons in DIS of muons on nucleons at COMPASS*, Ph.D. thesis, U. Mainz and U. Paris-Saclay (2019).
 - [11] A. Kwiatkowski, H. Spiesberger and H. J. Mohring, *Comput. Phys. Commun.* **69**, 155 (1992).
 - [12] A. Arbutov, D. Y. Bardin, J. Blümlein, L. Kalinovskaya and T. Riemann, *Comput. Phys. Commun.* **94**, 128 (1996).
 - [13] L. W. Mo and Y. S. Tsai, *Rev. Mod. Phys.* **41**, 205 (1969).
 - [14] D. Y. Bardin, C. Burdik, P. C. Khristova and T. Riemann, *Z. Phys. C* **42**, 679 (1989).
 - [15] R. Ent, B. W. Filippone, N. C. R. Makins, R. G. Milner, T. G. O’Neill and D. A. Wasson, *Phys. Rev. C* **64**, 054610 (2001).
 - [16] A. Afanasev, I. Akushevich, V. Burkert and K. Joo, *Phys. Rev. D* **66**, 074004 (2002).
 - [17] I. Akushevich and A. Ilyichev, *Phys. Rev. D* **100**, 033005 (2019).
 - [18] J. Blümlein and H. Kawamura, *Eur. Phys. J. C* **51**, 317 (2007).
 - [19] V. Bertone, M. Cacciari, S. Frixione and G. Stagnitto, *J. High Energy Phys.* **03** (2020) 135.
 - [20] J. Ablinger, J. Blümlein, A. De Freitas and K. Schönwald, *Nucl. Phys.* **B955**, 115045 (2020).
 - [21] J. C. Collins, D. E. Soper and G. F. Sterman, *Adv. Ser. Direct. High Energy Phys.* **5**, 1 (1989).
 - [22] S. Chekanov *et al.* (ZEUS Collaboration), *Eur. Phys. J. C* **21**, 443 (2001).
 - [23] H. Abramowicz *et al.* (H1 and ZEUS Collaborations), *Eur. Phys. J. C* **75**, 580 (2015).
 - [24] A. C. Benvenuti *et al.* (BCDMS Collaboration), *Phys. Lett. B* **223**, 485 (1989).

- [25] M. R. Adams *et al.* (E665 Collaboration), *Phys. Rev. D* **54**, 3006 (1996).
- [26] M. Arneodo *et al.* (New Muon Collaboration), *Nucl. Phys.* **B483**, 3 (1997).
- [27] A. Airapetian *et al.* (HERMES Collaboration), *J. High Energy Phys.* 05 (2011) 126.
- [28] V. Tvaskis *et al.*, *Phys. Rev. C* **81**, 055207 (2010).
- [29] G. C. Nayak, J.-W. Qiu and G. F. Sterman, *Phys. Rev. D* **72**, 114012 (2005).
- [30] While our calculation corresponds to the zero mass variable flavor scheme, it can also be extended to heavy quark schemes as in M. A. G. Aivazis, J. C. Collins, F. I. Olness and W. K. Tung, *Phys. Rev. D* **50**, 3102 (1994).
- [31] Note that studies of the QED structure of the electron have been made by a number of authors, including G. A. Miller, *Phys. Rev. D* **90**, 113001 (2014), X. Ji, A. Schäfer, F. Yuan, J.-H. Zhang and Y. Zhao, *Phys. Rev. D* **93**, 054013 (2016), A. Bacchetta, L. Mantovani and B. Pasquini, *Phys. Rev. D* **93**, 013005 (2016).
- [32] J. C. Collins and D. E. Soper, *Nucl. Phys.* **B194**, 445 (1982).
- [33] E. J. Williams, *Phys. Rev.* **45**, 729 (1934).
- [34] C. F. von Weizsäcker, *Z. Phys.* **88**, 612 (1934).
- [35] Y. L. Dokshitzer, *J. Exp. Theo. Phys.* **46**, 641 (1977).
- [36] V. N. Gribov and L. N. Lipatov, *Sov. J. Nucl. Phys.* **15**, 438 (1972).
- [37] L. N. Lipatov, *Sov. J. Nucl. Phys.* **20**, 94 (1975).
- [38] G. Altarelli and G. Parisi, *Nucl. Phys.* **B126**, 298 (1977).
- [39] N. Sato, C. Andres, J. J. Ethier and W. Melnitchouk, *Phys. Rev. D* **101**, 074020 (2020).
- [40] A. Accardi, L. T. Brady, W. Melnitchouk, J. F. Owens and N. Sato, *Phys. Rev. D* **93**, 114017 (2016).
- [41] J. C. Collins, D. E. Soper and G. F. Sterman, *Nucl. Phys.* **B250**, 199 (1985).
- [42] J. Collins and T. C. Rogers, *Phys. Rev. D* **96**, 054011 (2017).
- [43] L. Gamberg, A. Metz, D. Pitonyak and A. Prokudin, *Phys. Lett. B* **781**, 443 (2018).
- [44] T. Liu *et al.*, in preparation (2020).